Sensors and Actuators B 139 (2009) 447–452

Contents lists available at ScienceDirect

Sensors and Actuators B: Chemical

journal homepage: www.elsevier.com/locate/snb

Impedance spectroscopy analysis of TiO_2 thin film gas sensors obtained from water-based anatase colloids

M.A. Ponce [a], R. Parra [a,b], R. Savu [b,*], E. Joanni [b], P.R. Bueno [b], M. Cilense [b], J.A. Varela [b], M.S. Castro [a]

[a] Institute of Materials Science and Technology (INTEMA), CONICET – Universidad Nacional de Mar del Plata, B7608FDQ Mar del Plata, Argentina
[b] Instituto de Química, Universidade Estadual Paulista – UNESP, 14800-900 Araraquara, SP,Brazil

ARTICLE INFO

Article history:
Received 17 November 2008
Received in revised form 21 March 2009
Accepted 26 March 2009
Available online 7 April 2009

Keywords:
Titanium oxide
Thin films
Gas sensor
Impedance spectroscopy

ABSTRACT

In this work impedance spectroscopy technique was employed in order to characterize the gas-sensing behavior of undoped titanium dioxide (TiO_2) polycrystalline thin films. The electrical measurements were performed in a sensor-testing chamber that allows independent control of temperature, pressure, gas composition and flow rate. Frequency measurements, in the range from 40 Hz to 110 MHz, were performed in order to evaluate the gas sensor response of the samples as a function of temperature (50–350 °C) and surrounding atmosphere (vacuum or air at atmospheric pressure). Impedance spectroscopy is a very useful and important technique due to the possibility of using this method for discriminating between grain boundary capacitance (C_{gb}) and grain boundary resistance (R_{gb}) contributions. Therefore, a simple model taking into account variations in the intergranular potential barriers is proposed in this work.

1. Introduction

The increasing concern in the detection of toxic and flammable gases calls for the development of highly sensitive devices as well as for the understanding and determination of simplified models of sensor operation mechanisms. The interest has long been focused in wide band-gap semiconducting metal oxides such as SnO_2, ZnO and TiO_2, which suffer changes in the conductance when oxidizing or reducing species in air chemisorb onto the oxide particle or film surface [1,2]. In view of the importance in monitoring industrial, home and automobile pollution, today the development of nanostructured sensing films is not only an attractive trend toward miniaturization, but the alternative to maximize the surface-to-volume ratio and sensitivity [3].

Titanium dioxide has attracted much attention in the past decades and found applications of environmental interest in self-cleaning and energy efficient windows [4], dye-sensitized solar cells [5], photocatalysts for the degradation of water and air pollutants [6] and gas-sensing devices [7]. Moreover, the functionalization of titania mesoporous films is an interesting alternative toward highly selective bio-sensors [8]. TiO_2 presents two metastable polymorphs, anatase and brookite, and the stable phase rutile. Since the transition from anatase to rutile takes place at around 600–700 °C, rutile is the desired phase for high temperature applications (>800 °C) [7]. Anatase is characterized by high electron mobility responsible for its elevated sensitivity and faster response as a gas sensor [9]. Rutile and anatase exhibit further differences: the former is a p-type semiconductor while the latter shows n-type semiconductivity [10]. The n–p-transition regime for TiO_2 is displayed below 1200 K at oxygen partial pressures near atmospheric conditions. As far as the electronic properties are concerned, TiO_2 behaves in these conditions like an intrinsic semiconductor in which densities of electrons and holes are very similar. Therefore, a very low electronic conductivity must be expected. The loss of oxygen may be accompanied by the movement of Ti ions onto interstitial sites [11].

Significant advances have been achieved lately for the use of TiO_2 in gas-sensing devices. A great sensitivity to H_2 and ethanol has been found for undoped anatase films at 400 °C, whereas Sr, Tb and Y-doped films were barely sensitive to those gases [7,12]. The response of TiO_2 was also tested against NO_2, CO, ammonia, O_2 and water vapor, and the use of nanoscaled particles was observed to be critical in order to achieve sensitivity [3,13–17]. Anatase films on glass substrates also showed reproducibility and stability when exposed to CO at temperatures between 100 °C and 300 °C, apart from complete regeneration after the CO removal [18]. Akbar and co-workers discussed the electrical response of doped and undoped anatase gas sensors in several comprehensive papers [19–21]. They correlated the electrical properties with the microstructure and proposed, on the basis of *dc* and *ac* admittance spectroscopy measurements, an equivalent circuit that represents the grain boundary dominant response and considers trapping relaxations originated by the defects within the grain boundary region. The authors found consistency between the grain boundary *ac* response and changes

* Corresponding author. Tel.: +55 16 33016643.
E-mail address: raluk1978@yahoo.com (R. Savu).

0925-4005/$ – see front matter © 2009 Elsevier B.V. All rights reserved.
doi:10.1016/j.snb.2009.03.066

in the barrier thermal activation induced by the heat-treatment of TiO_2 bulk samples in the 700–900 °C temperature range [20]. The influence of additives such as Al [19], Fe [19,22], Y [19,20], Sr and Tb [7], Cr [23–25], Nb [13,24–28], Pt [9], Ta [13] and Li [29], on the performance of TiO_2-gas sensors has been extensively studied.

In this work, we report the fabrication of undoped-TiO_2 nanostructured films from sol–gel anatase colloids and their application as gas sensors. The films have a porous structure, being composed of small grains in the 20–40 nm range. The impedance spectroscopy technique was used in order to evaluate the electrical behavior of the samples under different atmospheres and temperatures. Our interpretation of the electrical response is slightly different from the one reported by Akbar and co-workers. The results allow us to explain the modifications in the intergranular potential barriers induced by different testing conditions and to contribute for a better understanding of the sensing mechanisms in anatase-based gas sensors.

2. Experimental details

In this work, $Ti(O^iPr)_4$ (97%, Aldrich) was mixed with acetic acid (100%, Merck) and a non-ionic surfactant (Triton X-100, Aldrich) in 2-propanol (Qhemis). Then, water was added dropwise, with stirring, in a 1:1 $Ti(O^iPr)_4$:H_2O molar ratio. The obtained gel was aged for 24 h in order to maximize condensation. The gel was peptized at 80 °C and the evaporated alcohol compensated with water. The resulting colloidal dispersion was transferred into a PTFE-lined stainless steel vessel for hydrothermal treatment at 200 °C. Afterwards, the dispersion was concentrated by evaporation until a 5 wt% TiO_2 paste was obtained. The paste was characterized by X-ray diffraction (XRD; Rigaku Rint2000) and thermal analysis (TG/DTA; Shimadzu TG50-DT50). The TiO_2 paste was doctor-bladed on insulating alumina substrates, onto which gold electrodes with an interdigitated shape had been previously sputtered, and films were heat-treated at 450 °C for 20 min. The morphology of the films was studied by field-emission scanning electron microscopy (FE-SEM; JEOL JSM 6700F).

For gas-sensing measurements, the films were tested in a chamber with temperature, pressure, gas composition and flow rate control. Electrical resistance and impedance measurements, in the 40 Hz–110 MHz frequency range, were carried out between 100 °C and 250 °C with an HP4192A impedance analyzer. The electrical behavior of the films was analyzed by means of impedance plots in which the impedance Z is shown in a complex plane with the reactance (Z'') plotted against the resistance (Z') [30]. The curves were obtained at different temperatures (25–350 °C), with heating and cooling rates of ~1 °C/min, in vacuum (10^{-2} Torr) and in dry air at atmospheric pressure. In order to ensure that the system was in steady state before data acquisition, it was verified that the response was constant in time. Fig. 1 describes the conditions of temperature and pressure as well as the procedure adopted for sequential measurements.

Due to the great electrical resistance of undoped-TiO_2 at low temperatures, semicircular curves were only obtained at temperatures higher than 330 °C. Thus, 350 °C was the selected temperature for the analysis. Finally, the electrical resistance and capacitance were determined from fittings of the impedance diagrams with an R(RC) equivalent circuit using the ZView 2.1 software.

3. Results and discussion

The XRD pattern of the TiO_2 colloid after hydrothermal treatment at 200 °C showed that the material crystallized exclusively into the anatase phase. As expected, no phase transition was observed after thermal treatments up to 600 °C. Thermal analyses indicated that organics were completely burned above 400 °C and that the phase transition to rutile takes place around 700 °C. Anatase is usually the desired phase in gas-sensing devices for service temperatures below 800 °C since electron mobility is higher in anatase than in rutile, leading to higher sensitivity and faster response [7,9]. Fig. 2 shows a FE-SEM image of a film heat-treated at 450 °C. The TiO_2 films are porous, consisting of small grains in the 20–40 nm range.

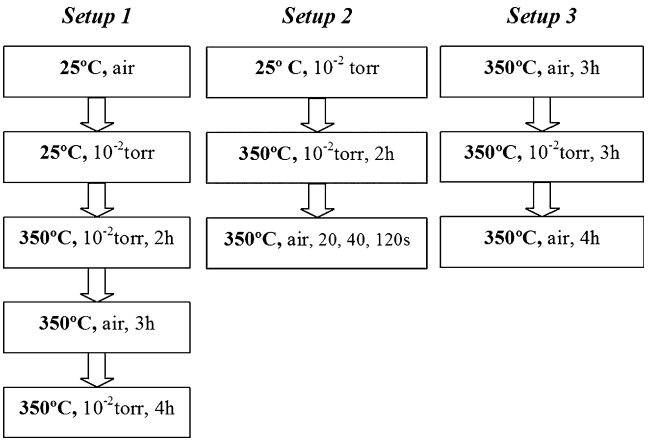

Fig. 1. Experimental procedure followed in Schedules 1, 2 and 3. Air was introduced at atmospheric pressure into the chamber.

The temporal response of the sensor (resistance vs. time curve) was recorded, from impedance spectroscopy measurements, when the atmosphere was changed from vacuum (10^{-2} Torr) to air (at atmospheric pressure) at a constant temperature of 350 °C, as shown in Fig. 3.

After a quick increase upon oxygen exposure, the electrical resistance measured at 40 Hz is almost constant after approximately 120 s. This phenomenon could be correlated with a significant diffusion of oxygen into the grain boundaries due to the open porous microstructure and the nanoscaled grain sizes. The film exhibited a very strong increase in resistance (almost three orders of magnitude) when air was introduced in the test chamber.

The results from impedance spectroscopy measurements, carried out according to the schedules shown in Fig. 1, can be fitted with a simple $R_b(R_{gb}C_{gb})$ electrical model where R_b and R_{gb} reflect the bulk and grain boundary resistances, respectively, and C_{gb} the capacitance across the grain boundary [31,32]. The impedance of a

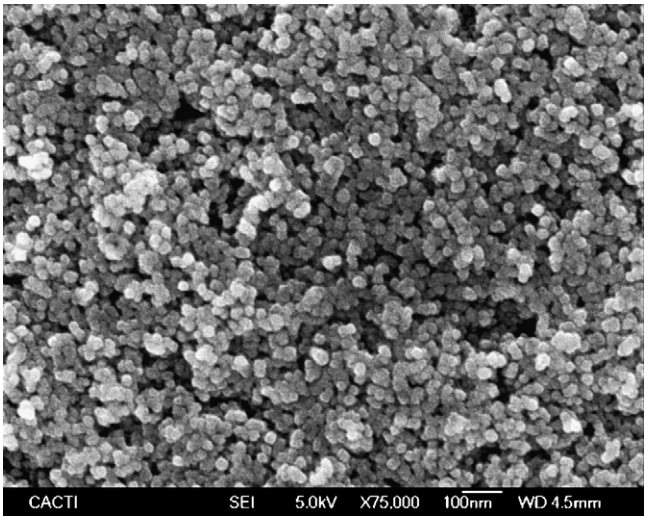

Fig. 2. FE-SEM image of a TiO_2 anatase film heat-treated at 450 °C.

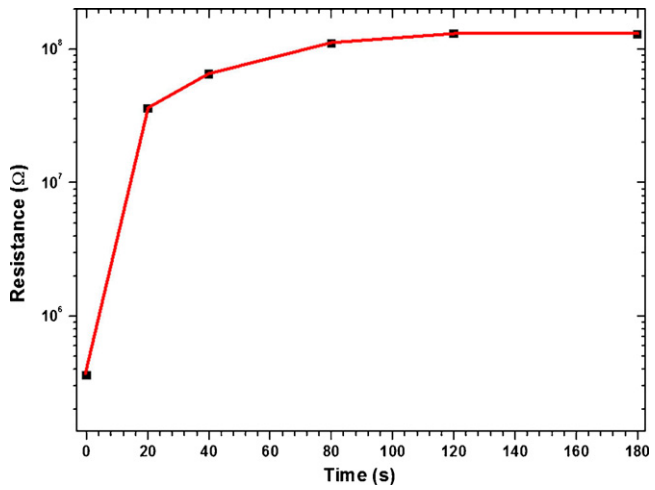

Fig. 3. Resistance vs. time curve recorded when the atmosphere was changed from vacuum (10^{-2} Torr) to air (at atmospheric pressure) at a constant temperature of 350 °C.

resistance R_{gb} in parallel with a capacitance C_{gb} is given by:

$$Z_{gb} = \frac{1}{R_{gb}^{-1} + j\omega C_{gb}}, \quad (1)$$

where $\omega = 2\pi f$.

Eq. (1) can be expressed as:

$$\left(\frac{Z'_{gb} - R_{gb}}{2}\right)^2 + Z''_{gb}{}^2 = \left(\frac{R_{gb}}{2}\right)^2 \quad (2)$$

where Z'_{gb} and Z''_{gb} are the real and imaginary components of Z_{gb}, respectively. The corresponding plot of the real against the imaginary component of Z_{gb} is a semicircle of radius $R_{gb}/2$ centered at $R_{gb}/2$. The addition of a series resistance R_b will only shift the curve in the R_b value. Thus, R_{gb} and R_b are derived from the low- and high-frequency resistance values, respectively, and the capacitance can be obtained from the maximum value of the reactance.

Fig. 4 shows the impedance plots registered at 350 °C according to Schedule 1 (Fig. 1).

When the sample is heated to 350 °C in vacuum (10^{-2} Torr), the impedance curves become measurable because of thermal activation. In presence of air at 350 °C (Fig. 4 filled circle) there is an

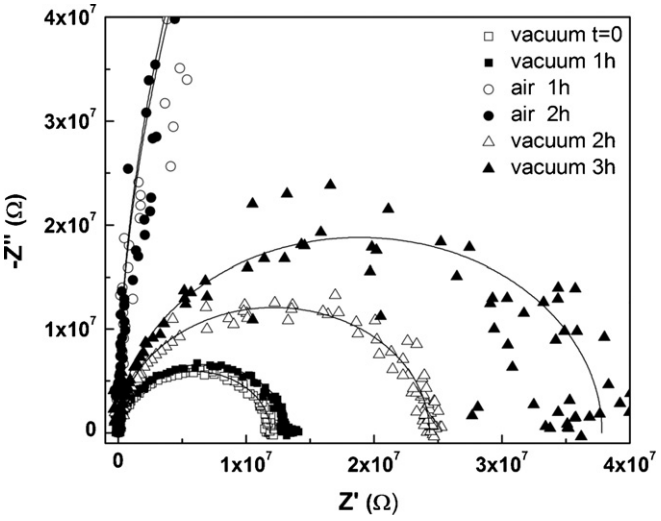

Fig. 4. Impedance spectroscopy curves of a sample treated according to Schedule 1.

increase in the grain boundary resistance due to oxygen adsorption at the particle surfaces, in agreement with n-type conductivity. This is depicted in the band diagrams of Fig. 5 by the transition from state a to state b. It is well known that the interaction of oxygen with grain surfaces produces the transfer of electrons from the bulk to the surface. From this process, the barrier height and the depletion width become larger and, as a consequence, the sample resistance increases. This leads to the barrier overlapping due to the larger depletion layer and to the alteration in the width of the potential barriers. This change can also be associated with the annihilation of vacancies due to the oxygen into-diffusion.

After 3 h the sample is exposed once again to vacuum, leading to the decrease in R_{gb} due to the lower barrier height, as shown in Fig. 5c. According to the generally accepted interpretation for electrical conduction in polycrystalline semiconductors, discrete energy levels within the band-gap are responsible for the formation of Schottky barriers at grain surfaces. Then, the negative charges due to chemisorbed oxygen at grain surfaces increase the Schottky potential energy barriers at the intergrains, having a pronounced effect on the electrical conductance. Subsequently, vacuum exposure induces oxygen desorption from the TiO_2 surface causing the decrease of the barrier heights and facilitating electrical conduction. However, the initial R_{gb} value is not completely recovered. This behavior can be understood if we consider the diffusion of oxygen and the fact that potential barriers reach new configurations of height and width. The oxygen adsorbed at the grain surfaces remain after evacuation of the chamber and its diffusion into the grains increase the barrier height of TiO_2 and annihilate oxygen vacancies, leading to wider depletion regions (Fig. 5c). Another consequence of these changes is the raising of the conduction band bottom ($V_a > V_c$) also shown in Fig. 5c. Here V_s is the surface barrier, which is the difference between the conduction band bottom at the surface E_{c_surf} and the conduction band bottom in the bulk E_{c_bulk}.

If there were non-overlapped potential barriers, both processes (adsorption and in-diffusion) would lead to a higher resistance: the diffusion at intergrains is much faster than the diffusion into the grains. However, when the intergranular barriers are overlapped and there is significant oxygen diffusion into the grains, affecting the concentration of oxygen vacancies and the Schottky barrier widths, the bottom of the barriers (and, consequently, the conductance) would be increased. This phenomenon it is known as unpinning of the Fermi level [32,35,36]. Conversely, if the barriers were previously overlapped (Fig. 5b and c) and vacuum is maintained for 2 h, the reverse process takes place as can be observed in Fig. 4 (open up-triangle) and in the band diagram of Fig. 5d. The out-diffusion of oxygen and the oxygen vacancy generation increase the sample resistance due to the decrease of the conduction band bottom from V_c to V_d. In the extreme situation of total decrease of the conduction band bottom, the Fermi level would be reached and qV would tend to Φ (where q is the absolute value of the electron charge and Φ is the barrier height) returning to the conditions in Fig. 5a. At this point, barriers would not be overlapped and the overlapping process would only be possible if oxygen would be introduced into the chamber (for temperatures above 300 °C). According to the Poisson equation, and due to the small particle size of the samples under study, the overlapping of depletion regions is highly probable. This is in agreement with results previously published by other researchers [33–35].

Fig. 6 shows the electrical response in air for the sample previously exposed to air and vacuum.

The figure shows the impedance curves after changing from vacuum to air ($t = 0$) at different times 20 s, 40 s and 120 s at 350 °C (Schedule 2, Fig. 1). Semicircles corresponding to measurements performed in air are larger than the ones previously obtained in

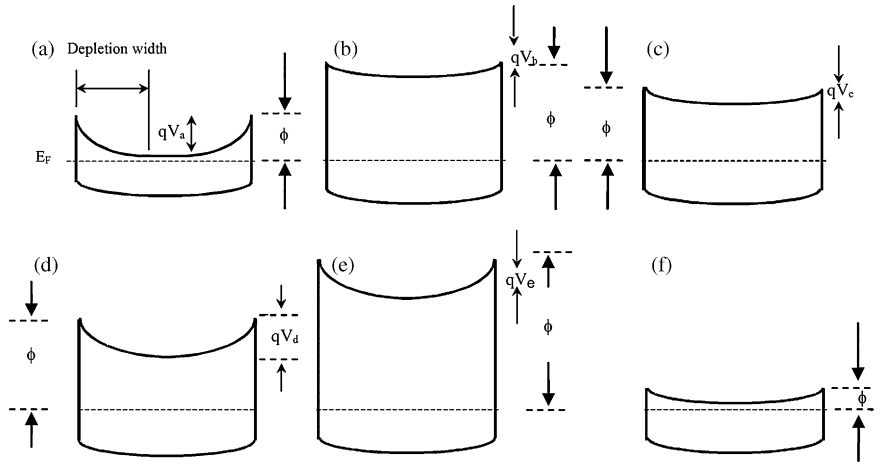

Fig. 5. Band diagram model showing changes in the interparticle potential barriers.

vacuum. This process can be interpreted on the basis of Fig. 5e. Due to the short stabilization time (120 s), a change from d to e is observed rather than a change from d to b. The oxygen adsorption at the grains surface increases the barrier height but there is not enough time for oxygen to diffuse into the TiO_2 grains. Finally, in order to promote overlapping the sample was cooled to 35 °C in air and heated once again to 350 °C in the same atmosphere during a 4 h process. The final configuration of the barriers corresponds to that of Fig. 5b and the sample was used for the following measurements.

Fig. 7 shows the impedance spectroscopy response during Schedule 3 (Fig. 1) carried out at 350 °C in air, then in vacuum and finally in air again. The average particle size of films annealed at 450 °C in air did not increase during measurements, as expected, due to the low temperature used for testing (350 °C).

The radii of semicircles became smaller in vacuum indicating that R_{gb}, as well as barrier height and width, decreased due to oxygen desorption (change from Fig. 5b to f). When the sample is exposed to air again, an increase in the sensitivity is clearly observed, due to the low initial R_{gb} at 350 °C. The curves in Fig. 7, fitted with an $R_b(R_{gb}C_{gb})$ equivalent circuit, yielded the resistance and capacitance values listed in Table 1. Notice the increase in R_{gb} after oxygen exposure (see also Fig. 4).

For Schottky barriers (samples with non-overlapped barriers), the capacitance is related to the electron concentration in the bulk,

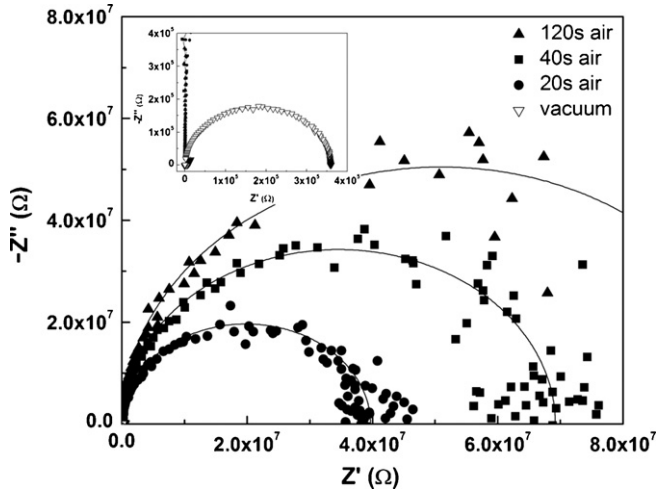

Fig. 6. Impedance spectroscopy curves of a sample treated according to Schedule 2.

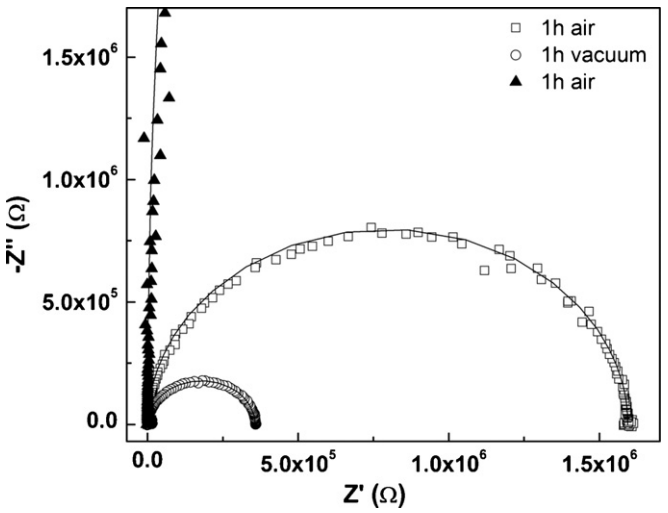

Fig. 7. Impedance spectroscopy curves of a sample treated according to Schedule 3.

Table 1
The resistance and capacitance values for the impedance spectroscopy curves registered during Schedule 3 measurements and fitted with an $R_b(R_{gb}C_{gb})$ equivalent circuit.

Schedule 3	Air (initial)	Vacuum	Air (final)
R_{gb} (Ω)	1.593×10^6	3.562×10^5	8.607×10^7
C_{gb} (F)	–	1.415×10^{-12}	1.215×10^{-12}

n, and to the barrier height, V_B, as [31]

$$C \propto \left(\frac{n}{V_B}\right)^{1/2}. \quad (3)$$

Therefore, because in the initial condition barriers are overlapped, C_{gb} is physically meaningful for the vacuum and for the final oxygen exposure conditions only. A decrease in the final capacitance is associated with a higher barrier and/or with a reduction of the donor concentration due to the annihilation of oxygen vacancies.

4. Conclusions

Impedance spectroscopy analysis of TiO_2 thin film gas sensors obtained from water-based anatase colloids was performed in this work. Hydrothermal treatment, at 200 °C, of the titanium colloidal

dispersion showed that the material crystallized exclusively into the anatase phase. TiO_2 doctor-bladed thin films heat-treated at 450 °C with nanoparticles in the 20–40 nm range were obtained. The sensor exhibited a good response time, with the electrical resistance being almost constant after approximately 120 s. The film exhibited a very strong increase in resistance (almost three orders of magnitude) when air was introduced in the test chamber. The impedance spectroscopy measurements performed on nanostructured anatase films were carried out in order to study the sensing mechanism at different atmospheres. The Schottky potential barrier height increased due to oxygen chemisorption at the intergrains, having a pronounced effect on the electrical n-type conductivity. Oxygen desorption from the TiO_2 surface due to vacuum exposure causes a decrease in the barrier height and facilitates electrical conduction.

Acknowledgements

This research was conducted with the financial support of CONICET (Argentina) and FAPESP and CNPq (Brazil). The authors are also grateful to Dr. P.M. Botta and the personnel at CACTI (Vigo University, Spain) for the FE-SEM session.

References

[1] N. Barsân, M. Schweizer-Berberich, W. Göpel, Fundamental and practical aspects in the design of nanoscaled SnO_2 gas sensors: a status report, Fresenius J. Anal. Chem. 365 (1999) 287–304.
[2] L. Mädler, T. Sahm, A. Gurlo, J.-D. Grunwaldt, N. Barsân, U. Weimar, S.E. Pratsinis, Sensing low concentrations of CO using flame-spray-made Pt/SnO_2 nanoparticles, J. Nanopart. Res. 8 (2006) 783–796.
[3] I.-D. Kim, A. Rothschild, B.H. Lee, D.Y. Kim, S.M. Jo, H.L. Tuller, Ultrasensitive chemiresistors based on electrospun TiO_2 nanofibers, Nano Lett. 6 (2006) 2009–2013.
[4] A. Werner, A. Roos, Condensation tests on glass samples for energy efficient windows, Sol. Energy Mater. Sol. Cells 91 (2007) 609–615.
[5] B. O'Regan, M. Grätzel, A low-cost, high-efficiency solar cell based on dye-sensitized colloidal TiO_2 films, Nature 353 (1991) 737–739.
[6] H. Choi, Y.J. Kim, R.S. Varma, D.D. Dionysiou, Thermally stable nanocrystalline TiO_2 photocatalysts synthesized via sol-gel methods modified with ionic liquid and surfactant molecules, Chem. Mater. 18 (2006) 5377–5384.
[7] H. Tang, K. Prasad, R. Sanjinés, F. Levy, TiO_2 anatase thin films as gas sensors, Sens. Actuators B: Chem. 26–27 (1995) 71–75.
[8] M.C. Fuertes, G.J.A.A. Soler-Illia, Processing of macroporous titania thin films: from multiscale functional porosity to nanocrystalline macroporous TiO_2, Chem. Mater. 18 (2006) 2109–2117.
[9] M. Epifani, A. Helwig, J. Arbiol, R. Díaz, L. Francioso, P. Siciliano, G. Mueller, J.R. Morante, TiO_2 thin films from titanium butoxide: synthesis, Pt addition, structural stability, microelectronic processing and gas-sensing properties, Sens. Actuators B: Chem. 130 (2008) 599–608.
[10] N. Savage, B. Chwieroth, A. Ginwalla, B.R. Patton, S.A. Akbar, P.K. Dutta, Composite n-p semiconducting titanium oxides as gas sensors, Sens. Actuators B: Chem. 79 (2001) 17–27.
[11] A.J. Moulson, J.M. Herbert, Electroceramics, Chapman & Hall, London, 1990.
[12] L.A. Harris, A titanium dioxide hydrogen sensor, J. Electrochem. Soc. 127 (1980) 2657–2662.
[13] E. Traversa, M.L. Di Vona, S. Licoccia, M. Sacerdoti, M.C. Carotta, M. Gallana, G. Martinelli, Sol–gel nanosized semiconducting titania-based powders for thick-film gas sensors, J. Sol–Gel Sci. Technol. 19 (2000) 193–196.
[14] I.-D. Kim, A. Rothschild, D.-J. Yang, H.L. Tuller, Macroporous TiO_2 thin film gas sensors obtained using colloidal templates, Sens. Actuators B, Chem. 130 (2008) 9–13.
[15] B. Karunagaran, P. Uthirakumar, S.J. Chung, S. Velumani, E.-K. Suh, TiO_2 thin film gas sensor for monitoring ammonia, Mater. Charact. 58 (2007) 680–684.
[16] M.R. Mohammadi, D.J. Fray, M.C. Cordero-Cabrera, Sensor performance of nanostructured TiO_2 thin films derived from particulate sol–gel route and polymeric fugitive agents, Sens. Actuators B: Chem. 124 (2007) 74–83.
[17] D. Mardare, N. Iftimie, D. Luca, TiO_2 thin films as sensing gas materials, J. Non-Cryst. Solids 354 (2008) 4396–4400.
[18] A. Al-Homoudi, J.S. Thakur, R. Naik, G.W. Auner, G. Newaz, Anatase TiO_2 films based CO gas sensor: film thickness, substrate and temperature effects, Appl. Surf. Sci. 253 (2007) 8607–8614.
[19] L.D. Birkefeld, M.A. Azad, S.A. Akbar, Carbon monoxide and hydrogen detection by anatase modification of titanium dioxide, J. Am. Ceram. Soc. 75 (1992) 2964–2968.
[20] A.M. Azad, L.B. Youdunan, S.A. Akbar, M.A. Alim, Characterization of TiO_2-based sensor materials using immittance spectroscopy, J. Am. Ceram. Soc. 77 (1994) 481–486.
[21] P.K. Dutta, A. Ginwalla, B. Hogg, B.R. Patton, B. Chwieroth, Z. Liang, P. Gouma, M. Mills, S. Akbar, Interaction of carbon monoxide with anatase surfaces at high temperatures: optimization of a carbon monoxide sensor, J. Phys. Chem. B 103 (1999) 4412–4422.
[22] E. Rezlescu, C. Doroftei, N. Rezlescu, P.D. Popa, Preparation, structure and gas-sensing properties of γ-Fe_2O_3 and γ-Fe_2O_3-TiO_2 thick films, Phys. Status Solidi (a) 205 (2008) 1790–1793.
[23] E. Alessandri, E. Comini, G. Bontempi, L.E. Faglia, G. Depero, Sberveglieri, Cr-inserted TiO_2 thin films for chemical gas sensors, Sens. Actuators B: Chem. 128 (2007) 312–319.
[24] R.K. Sharma, M.C. Bhatnagar, Improvement of the oxygen gas sensitivity in doped TiO_2 thick films, Sens. Actuators B: Chem. 56 (1999) 215–219.
[25] K. Zakrzewska, Gas sensing mechanism of TiO_2-based thin films, Vacuum 74 (2004) 335–338.
[26] M.C. Carotta, M. Ferroni, V. Guidi, G. Martinelli, Preparation and characterization of nanostructured titania thick films, Adv. Mater. 11 (1999) 943–946.
[27] M. Ferroni, M.C. Carotta, V. Guidi, G. Martinelli, F. Ronconi, O. Richard, D. Van Dyck, J. Van Landuyt, Structural characterization of Nb-TiO_2 nanosized thick-films for gas sensing application, Sens. Actuators B: Chem. 68 (2000) 140–145.
[28] G.S. Devi, T. Hyodo, Y. Shimizu, M. Egashira, Synthesis of mesoporous TiO_2-based powders and their gas-sensing properties, Sens. Actuators B: Chem. 87 (2002) 122–129.
[29] M.L. Zhang, Z.H. Yuan, C. Zheng, Fast response of undoped and Li-doped titania thick-films at low temperature, Sens. Actuators B: Chem. 131 (2008) 680–686.
[30] P.T. Moseley, Solid state gas sensors, Meas. Sci. Technol. 8 (1997) 223–237.
[31] M. Seitz, F. Hampton, W. Richmond, in: M.F. Yan, A.H. Heuer (Eds.), Influence of Chemisorbed Oxygen on the ac Electrical Behavior of Polycrystalline ZnO. Advances in Ceramics, vol. 7, The American Ceramic Society Inc., Ohio, 1983, pp. 60–70.
[32] M.A. Ponce, M.S. Castro, C.M. Aldao, Influence of oxygen adsorption and diffusion on the overlapping of intergranular potential barriers in SnO_2 thick-films, Mater. Sci. Eng. B 111 (2004) 14.
[33] M.J. Madou, S.R. Morrison, Chemical Sensing with Solid State Devices, Academic Press, Boston, 1989.
[34] X. Wang, S.S. Yee, W.P. Carey, Transition between neck-controlled and grain-boundary-controlled sensitivity of metal-oxide gas sensors, Sens. Actuators B: Chem. 24–25 (1995) 454–457.
[35] C. Malagù, M.A. Ponce, C.M. Aldao, G. Martinelli, Unpinning of the Fermi level and tunnelling in metal oxide semiconductors, Appl. Phys. Lett. 92 (2008) 162104.
[36] G. Blaustein, M.S. Castro, C.M. Aldao, Influence of the frozen distributions of oxygen vacancies on tin oxide conductance, Sens. Actuators B: Chem. 55 (1999) 33–37.

Biographies

M.A. Ponce Obtained his BSc in Chemistry in 1999 and PhD in Material Science in 2005 from Mar del Plata National University (UNMdP), Argentina. Since April 2007 he works as assistant researcher at CONICET-INTEMA, UNMdP. His current research interest includes the development of electronic conduction mechanism of functional inorganic materials.

R. Parra Received his PhD in Materials Science in 2006 from the University of Mar del Plata (UNMdP). He then spent two years as a postdoctoral research fellow at Chemistry Institute, UNESP-Araraquara, and is currently employed as an assistant researcher of CONICET at INTEMA, UNMdP. He is concerned with the chemical synthesis and characterization of inorganic materials for electroceramic devices.

R. Savu Graduated as Physical Engineer at Bucharest University, Faculty of Physics, Section of Technological Physics, in June 2001. She is a now a PhD student at PosMat, UNESP Bauru, Brazil, developing the experimental part of her project at Chemistry Institute, Araraquara, Brazil. Her research is focused on nanostructure based gas sensors and photodetectors.

E. Joanni Has a PhD degree from the University of Sheffield (1990). He is currently a researcher at UNESP Araraquara, Brazil. His main interests are in thin film deposition by physical methods, nanostructures, semiconducting oxides, dielectrics, sensors and memories.

P.R. Bueno Received his PhD in Physical Chemistry in 2003 from Federal University of São Carlos, Brazil. He did his postdoctoral research in Physics and Mathematics at São Paulo University in 2004 and nowadays he is Assistant Professor at UNESP Araraquara, Brazil. His research is focused onto frequency response techniques applied in different fields, such as semiconductors, electrochemistry and biosensor devices.

M. Cilense He graduated in Pharmacy in 1961 and received his PhD degree in 1968 at São Paulo University, Brazil. He was a titular professor at Araraquara Chemistry Institute – UNESP until 2003, recently being a volunteer professor at the same institution. He has experience in areas of Materials Science and Engineering and Metallurgy,

with emphases in phase transformation processes. His main interests are in tin oxide based varistors, ferroelectrics and electronic ceramics.

J. A. Varela Has a PhD degree from the University of Washington (1981). He is a Professor at UNESP Araraquara, Brazil. He is also the Vice-President of FAPESP and member of the International Academy of Ceramics, taking part of the editorial board for: Ceramics International, Science of Sintering, Cerâmica and Materials Research. He has wide experience in the area of Materials Science and Engineering, with emphasis in ceramics, working mainly on thin films, ferroelectric materials, dielectrics, varistors, grain boundary properties and sintering.

M.S. Castro Obtained her Chemical Engineering degree in 1988, and PhD in Materials Science in 1993 from Mar del Plata National University. Her current research interests include the development and application of functional inorganic materials.